

# Marine Current Turbine Imbalance Fault Detection Method Based on Angular Resampling

Tao Xie\*, Tianzhen Wang \*\*, Demba Diallo\*\*\*

\*Department of Electrical Automation, Shanghai Maritime University, Shanghai, (Tel: 021-38282624; e-mail:

\*smu\_taoxie@163.com, \*\*wtz0@sina.com).

\*\*\*University of Paris-Sud, France, (demba.diallo@geeps.centralesupelec.fr)

---

**Abstract:** Marine current power generation is increasingly attracting worldwide attention. However, mechanical imbalance fault often occurring when MCT blades are biofouled or corroded. This is a challenging problem due to the varying shaft rotating frequency (SRF) generate by the variable current flow. To deal with the imbalance fault, an angular resampling method based on the instantaneous power signal is proposed. This method monitors the output power of a variable-speed MCT generator and first processes the data using an angular resampling algorithm is to obtain a stationary signal. In the second step, a low-pass filter removes high frequencies and extract the fault characteristic. The simulation and the experiments verify the effectiveness of the proposed method for the MCT imbalance faults. The comparison with the motor current or voltage signature analysis has shown its superiority in terms of sensitivity to fault severity.

*Keywords:* Marine current turbine (MCT); imbalance fault detection; power signal; angular resampling.

---

## 1. INTRODUCTION

The marine energy has been paid more and more attention by countries all over the world due to the increasingly serious world energy crisis [1]. However, the complexity of the marine environment and plankton in seawater are important factors that interfere with the normal operation of MCT, particularly regarding maintenance and monitoring costs. Indeed, mechanical imbalance fault is one of the most significant of MCTs fault. Therefore, effective imbalance fault detection is essential.

Some reviews proposed that the instantaneous power signal can monitor stator winding asymmetry fault [2], indeed, it also work with blade imbalance fault [3]. Nevertheless, most of the existing research focused on the use of vibration data to monitoring the MCT condition. The author in [4] used an analysis of vibration signals, ultimately successful detection of the imbalanced fault of MCT. However, the vibration sensors are inevitably subject to failure, which could increase the maintenance cost for the whole MCT monitoring system. Also, vibration signal combined with stator current signal, for blade imbalance [5] or air gap eccentricity detection also has a good performance in practice [6]. The author in [7] proposed resampling and the EMD method to detect the MCT imbalanced fault. In [8], the d-q coordinate transformation method has been used to find the fault features, based on the stator 3-phase current measurement three phases stator current.

The generator output instantaneous power has also been used to monitor conditions [9], it may contain more information because it includes the features of voltage and current in the different conditions [10]. An image processing technology

based on power signal is proposed in [11], to monitor the state of turbine blades, and this method requires high resolution of the output power signal image of the generator. An approach for turbine output power signal pre-processing has been proposed in [12], can effectively remove the high-frequency interference part of instantaneous power. In [13], the wavelet transform method is presented for instantaneous power signal processing, but the case of variable SRF is obviously not considered.

This paper presents a fault detection method which is angular resampling based on the instantaneous output power of MCT generator. The proposed method obtains the variable instantaneous power from the MCT generator terminal, then using the angular resampling method transfer the variable characteristic frequencies of blade imbalance faults to a constant one. Finally, a low-pass filter is designed to filter high frequencies. The experimental results show that the proposed method can solve problems such as inconspicuous fault characteristics caused by the variable marine current in the direct-drive MCT system.

## 2. PROBLEMS DESCRIPTION

### 2.1 Variable marine current with turbulence

The structure of MCT is similar to WT, but the condition monitoring of MCT needs to be considered more comprehensively because the variable marine current and the more complex seabed environment. For ease of understanding, some concepts are described in Fig 1.

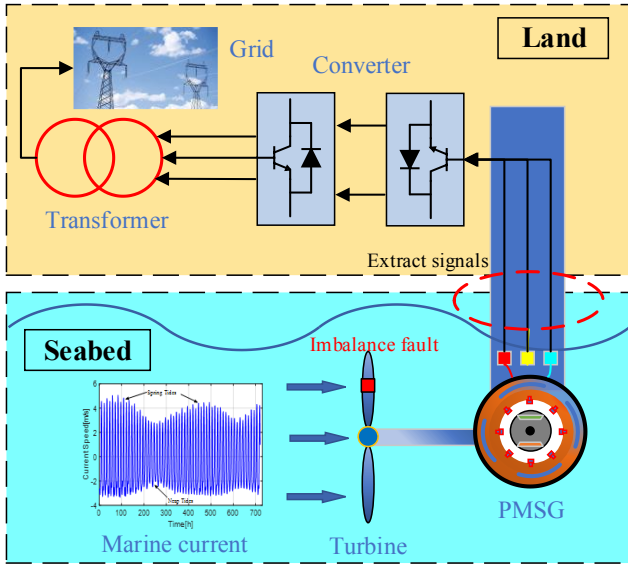


Fig. 1. Examples of marine current turbine concepts.

Marine current is not constant, which makes the MCT generator output power variable [14]. Due to the high density of marine current and the influence of turbulence, the instantaneous power fluctuates widely.

## 2.2 MCT Blade mass imbalance fault

In addition to surges and turbulence, plankton and marine sediments settle on MCT blades, resulting in mass imbalance fault. When MCT is operating in balanced condition, the stator current of one of phase can be expressed as:

$$i(t) = I_{\max} \cos(\omega_e t) \quad (1)$$

where  $I_{\max}$  is maximum value of the fundamental supply current;  $\omega_e = 2\pi f_e$ , is stator supply angular frequency. The stator voltage in phase one is:

$$u(t) = U_{\max} \cos(\omega_e t + \varphi) \quad (2)$$

where  $U_{\max}$  is maximum value of the fundamental supply voltage;  $\varphi$  is initial phase angle.

Hence, the corresponding instantaneous power of MCT generator in healthy case can be expressed as:

$$P(t) = u(t)i(t) = 0.5U_{\max}I_{\max} \cos(\varphi) + 0.5U_{\max}I_{\max} \cos(2\omega_e t - \varphi) \quad (3)$$

It's possible to verify that the instantaneous power in a healthy case includes two components, one is the DC component, the other one is the double current frequency from (3).

A mass imbalance fault of MCT leads to an asymmetry between the rotor and stator of generator. Thus, in the case of imbalanced fault, the stator current of one phase becomes [15]

$$i_{im}(t) = I_{\max} \cos(\omega_e t) + \frac{I_b}{2} \sin[(\omega_e + \omega_m)t] + \frac{I_b}{2} \sin[(\omega_e - \omega_m)t] \quad (4)$$

And the stator voltage:

$$u_m(t) = U_{\max} \cos(\omega_e t + \varphi) + \frac{U_b}{2} \sin[(\omega_e + \omega_m)t + \varphi] + \frac{U_b}{2} \sin[(\omega_e - \omega_m)t + \varphi] \quad (5)$$

Where  $I_b$  and  $U_b$  are maximum values of sideband on both sides of the main frequency, respectively. Hence, the maximum values is depend on the fault severity.

In the case of corresponding fault case, the equation for instantaneous power one of phase is given by:

$$P_m(t) = i_{im}(t)u_m(t) = 0.5U_{\max}I_{\max} \cos(\varphi) + 0.5U_{\max}I_{\max} \cos(2\omega_e t - \varphi) + 0.25(2U_bI_{\max} + U_{\max}I_b)[\sin((2\omega_e + \omega_m)t + \varphi) + \sin((2\omega_e - \omega_m)t - \varphi)] + 0.25U_bI_b[\cos((2\omega_e + 2\omega_m)t + \varphi) + \cos((2\omega_e - 2\omega_m)t - \varphi)] + 0.25U_bI_b[\cos(2\omega_e t + \varphi) + \cos(2\omega_e t - \varphi)] + -0.25U_bI_b[\cos(2\omega_m t + \varphi) + \cos(2\omega_m t - \varphi)] + 0.25(2U_bI_{\max} + U_{\max}I_b)[\sin(\omega_m t + \varphi) + \sin(\omega_m t - \varphi)] \quad (6)$$

Compared with (3), besides the average component  $DC$  and fundamental frequency  $2f_e$  with the sideband, it also contains additional components at frequency  $f_m$ . In addition, because the amplitude of the  $2f_m$  frequency is small, it can be neglected. Thus, in the proposed method, the presence of mass imbalance fault of MCT is characterized by the increase in the fault frequencies  $f_m$ , which is an excitation in SRF. Hence, the excitation at 1P frequency can be used as the fault feature of imbalanced fault detection for MCT.

However, when using SPF to identify faults, it should also be noted that SPF variable with the current rate, so the non-stationary signal should be converted into stationary. At the same time, it can be found from the (6) that there is still a  $2f_e$  frequency in the spectrum, so it is still necessary to choose an appropriate filter to filter out the double frequency.

## 3. FAULT FEATURE EXTRACTED BASED ON ANGULAR RESAMPLING METHOD

One stator phase current (e.g.  $i_{sa}$ ), and one stator phase voltage (e.g.  $u_{sa}$ ) are measured to calculate the instantaneous electrical power to extract the fault frequency, this power should be processed. However, because of the variable marine current velocity and the turbulence, the instantaneous power signal is non-stationary, therefore classical spectrum analysis could not be applied.

### 3.1 Angular resampling of the instantaneous power

The frequent change of marine current velocity leads to variable instantaneous power. Also, the rotation frequency of the MCT generator changes within a certain range, if the instantaneous power signal is not processed, the fault feature extraction will be interfered. This method obtains the step size of resampling through constant angle interval, to successfully sample the stable MCT instantaneous power. After resampling, the fault frequency excitation in SRF will become constant. The graphs displayed in Fig.2 show how the resampling transforms the initial non-stationary power signal to a stationary one.

The key of this method is calculate the variable-step, here, the instantaneous phase of power can be use in this case.

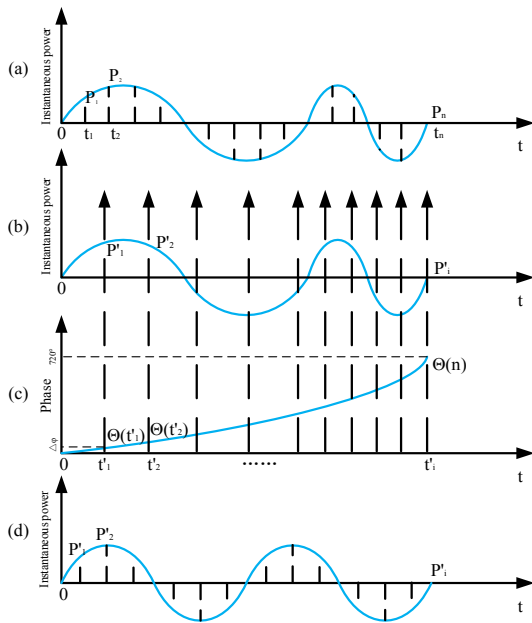


Fig. 2. (a) and (b) An instantaneous power of MCT with fix sample frequency (c) The instantaneous phase of power (d) a uniformly sampled instantaneous power of MCT.

The Hilbert transform of MCT instantaneous power  $P(t)$ , denoted by  $H[P(t)]$ , can be expressed as:

$$H[P(t)] = \frac{1}{\pi} \int_{-\infty}^{\infty} \frac{P(\tau)}{t - \tau} d\tau \quad (7)$$

The instantaneous phase of MCT power is estimated from the analytic signal as:

$$\theta(t) = \arctan \left[ \frac{H[P(t)]}{P(t)} \right] \quad (8)$$

Also, the instantaneous phase of MCT power, which is denoted as  $\theta(t)$  in term to frequencies, is defined as:

$$\theta(t) = 2\pi \int^t 2f_e(\tau) + f_m(\tau) dt \quad (9)$$

Meanwhile, if the the maximum value of the phase is  $\theta_{angle\max}$ , an equal phase increment can be divided as follows:

$$\Delta\theta = \frac{\theta_{angle\max}}{L_s p} \quad (10)$$

where  $L_s$  is a constant value that determines the number of sampling points as shown in Fig.2;  $\theta_{angle\max}$  is maximum value of the instantaneous phase. The calculated variable-step series will be used to resample the new fault characteristic signal. The current instantaneous power signal can be obtained by variable-step interpolation as follows.

$$t'_n = t_i + \frac{t_{i+1} - t_i}{\theta_{i+1} - \theta_i} (\theta_n - \theta_i) \quad (11)$$

$$P'_n = P_i + \frac{P_{i+1} - P_i}{t_{i+1} - t_i} (t'_n - t_i) \quad (12)$$

where  $t'_n$  and  $P'_n$  is the variable sampling step and new stationary instantaneous power signal, respectively;  $t_i$  and  $\theta_i$  is the original sampling time and the phase of instantaneous power signal, and  $\theta_n$  is the constant of equal-interval phase. After variable step resampling, the fault frequency  $f_m$  contained in the instantaneous power signal is converted to a constant value.

### 3.2 Description of the fault detection method

The proposed method pre-processed the MCT calculated instantaneous power and to extract fault features, is implemented in the following steps as shown in Fig. 3.

- 1) It starts with non-stationary instantaneous power.
- 2) Angular resampling transforms the signal into stationary one.
- 3) A low-pass filter is used for handle with high frequency components.
- 4) The frequency analysis is done to extract the mass imbalance signature.

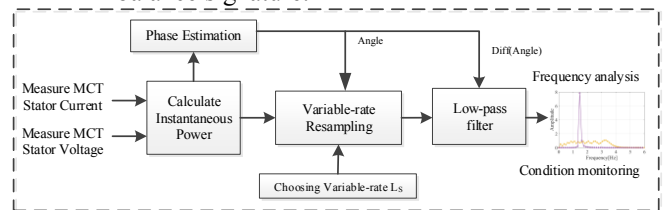


Fig. 3. Block diagram of proposed method.

## 4. SIMULATION AND EXPERIMENT RESULTS

### 4.1 Simulation results

To verify the angular resampling method based on instantaneous power for mass imbalance fault detection, a simulation model is built in Matlab/Simulink as shown in Fig.4. It includes the MCT, the permanent magnet synchronous generator, the imbalance fault generation module and the load.

To better reflect reality, the generation of wave and turbulence is added with a marine current velocity varying between 1.2 to 1.5 m/s. The sampling frequency is set at 1 kHz.

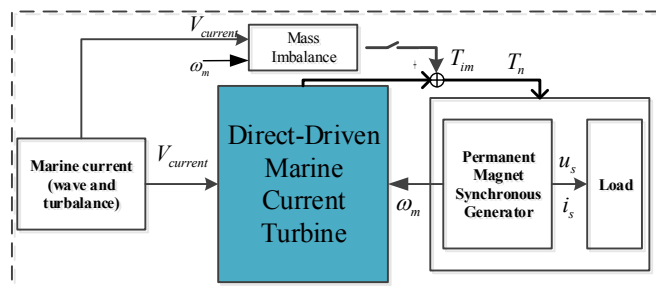


Fig. 4. Structure of MCT Simulink model

Three fault scenarios are simulated with additional mass equal to 1%, 2%, and 3% of blade. Fig.5 shows the positive effect of the instantaneous power with a step size  $L_s$  set as 8 and the low-pass filtering. It's clear that with the proposed method the fault characteristic frequency (frequency rotation) is stable at 2Hz ( $f_e = 16\text{Hz}$ ) after angular resampling and filtering.

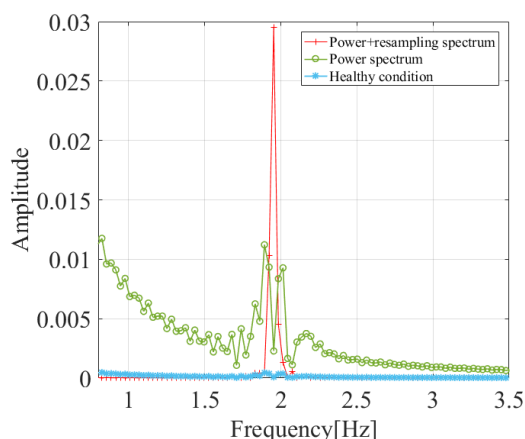


Fig.5. Comparison of the frequency spectrum in shaft rotation frequency.

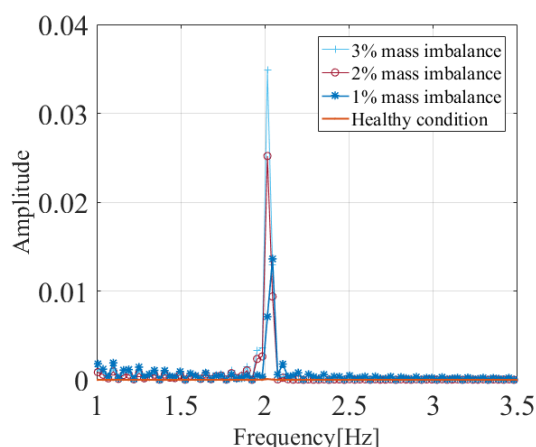


Fig.6. Power spectrum for different fault severities.

Fig.6 displays the transformed instantaneous power spectrum for different operating condition. One can first

notice that in healthy condition there is no excitation in SPF. One can also notice that the 1P frequency amplitude increases with the fault severity.

#### 4.2 Experimental results

The proposed method is now being evaluated with a 230W direct-drive PMSG experimental platform was built. The MCT generator is placed in the water flow channel as shown in Fig. 7.



Fig. 7. Current tunnel with MCT and data acquisition system.



Fig. 8. Blade with rope to create a mass imbalance condition.

The simulated current flow rate is regulated by the variable frequency regulator of the pump motor, and the adjustment range is from 0.9m/s to 1.5m/s. The measured stator current and voltage signals are collected by condition monitoring platform which equipped with corresponding acquisition card. The role of the drum motor is to simulate the waves, so that the turbulence of the current in the experiment changes with the same pump flow rate.

Table I. The detailed parameters of the MCT system

The prototype parameters			
Airfoil	Naca0018	Number of pole pairs	8
Pitch Angle(deg)	3.4-25.2	Flux (Wb)	0.1775
Blade width(m)	0.06	Resistance( $\Omega$ )	3.3
Sweep radius(m)	0.3	d-q axis inductance(mH)	11.873

In order to create a mass imbalance fault, a rope of known quality is wound around the blades of the current generator as an attachment is illustrate in Fig. 8. One blade has an

additional mass compare with other two. To keep constant fault centre frequency, the pump frequency is adjusted so that the power frequency does not change for the corresponding imbalanced fault test.

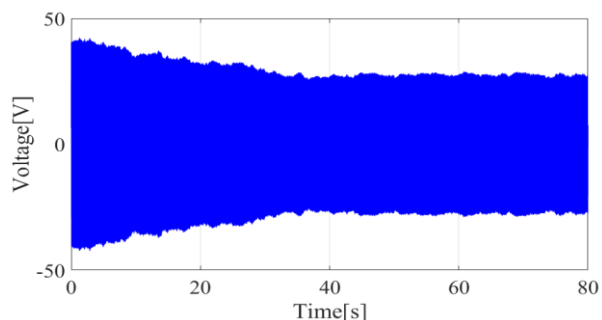


Fig.9. The time domain waveform of the voltage.

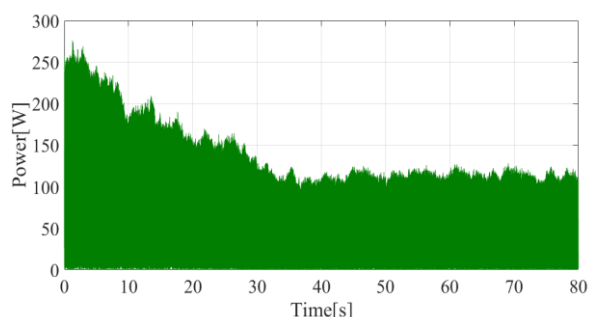


Fig.10. The time-domain waveform of the instantaneous power.

Fig.9 shows the time-domain waveform of the voltage and Fig.10 shows the time-domain waveform of the instantaneous power, the stator voltage and instantaneous power is variable when water flow is change.

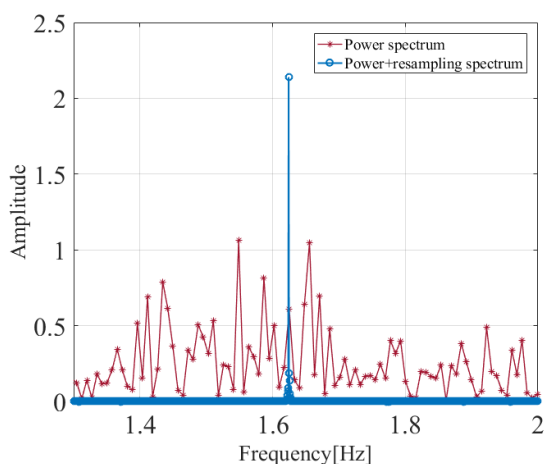


Fig.11. Comparison of the frequency spectrum in shaft rotation frequency.

The proposed angular resampling with low-pass filter method was applied to the instantaneous electrical power of MCT. Fig.11 shows the power spectrum with and without angular resampling. It's clear that with the proposed method the fault characteristic frequency (frequency rotation) is

stable at 1.62Hz ( $f_e = 12.96\text{Hz}$ ) after angular resampling and filtering. In the following, only the resampling instantaneous electrical power will be analysed. In Fig.12, we have plotted its power spectrum for three different fault severities.

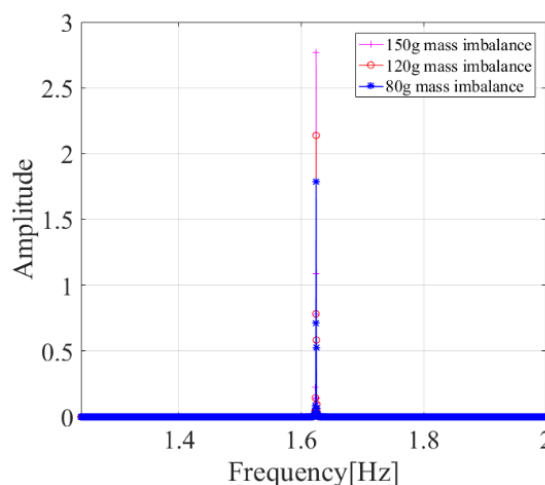


Fig.12. Comparison of the frequency spectrum for different fault severities

At a constant flow rate, Fig.13 shows a comparison of the amplitude of fault characteristics using different signal sources. At the same time, the current signal and the voltage signal are compared. Fig.14 shows the amplitude of fault characteristics from three signals for different marine current speeds under a constant additional mass ( $M_2$ ).

From these two figures, three conclusions can be drawn as following:

- 1) The resampled power spectrum is much more sensitive to the fault severity.
- 2) The resampled power spectrum is insensitive than the current and the voltage to the variable marine current velocity.
- 3) The resampled power enhances the fault feature and improves the degree of fault feature extraction.

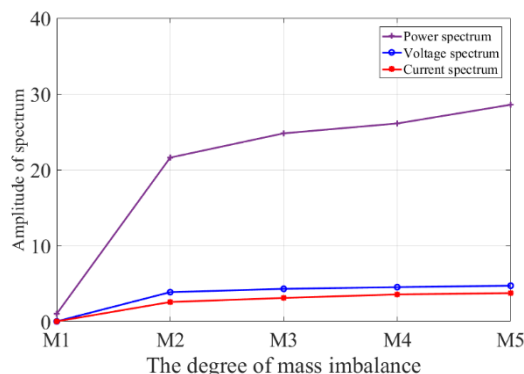


Fig.13 1P-frequency amplitude of spectrum under different degrees of mass imbalance (M1: healthy case, M2: additional mass 60g, M3: 80g, M4: 120g, M5: 150g).

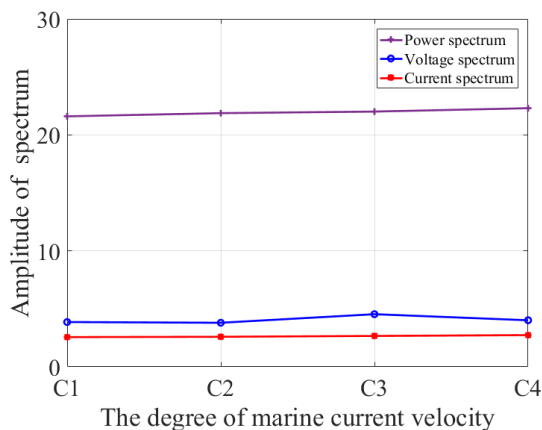


Fig.14 1P-frequency amplitude of spectrum for different flow velocities (C1:0.95m/s, C2: 1.1m/s, C3: 1.2m/s, C4: 1.3m/s, under additional mass: M2).

## 5 CONCLUSIONS

In this paper, a method of angular resampling to detect the imbalance fault of MCT by using the generator instantaneous output power has been presented. The method is composed of here steps:

- 1) Computation of the instantaneous output power from the measured stator current and voltage;
- 2) Resampling and low-pass filtering to convert the non-stationary power signal into a stationary one despite the variable marine current flow velocity and turbulence;
- 3) Extracting of the 1P frequency amplitude as the imbalance fault characteristic.

The simulation and the experimental results have shown that this resampling instantaneous generator output power is a sensitive and robust imbalance fault indicator.

## REFERENCES

1. Aggidis, G.A. Taylor, C.J. (2017). Overview of wave energy converter devices and the development of a new multi-axis laboratory prototype, *IFAC-PapersOnLine*, vol. 50, pp. 15651-15656.
2. Ma, H. Zhang, Z. Ju, P. (2015). Stator fault detection of doubly-fed induction generators using rotor instantaneous power spectrum. *IEEE International Symposium on Diagnostics for Electrical Machines. IEEE*.
3. Yang, T. Ren, Y. Liu, X. (2012). Research on the modelling and simulation of wind turbine rotor imbalance fault. *Journal of Mechanical Engineering*, vol. 48(6), pp.130-135.
4. Duhaney, J. Khoshgoftaar, T. Wald, R. (2012). Applying Feature Selection to Short Time Wavelet Transformed Vibration Data for Reliability Analysis of an Ocean Turbine, in: *Machine Learning and*

- Applications (ICMLA), *2012 11th International Conference* pp. 330-337.
5. Cheng, F. Qiu, L. Qiao, W. (2018). Fault Diagnosis of Wind Turbine Gearboxes Based on DFIG Stator Current Envelope Analysis. *IEEE Transactions on Sustainable Energy*, pp. 1-1.
6. Alameh, K. Cité, N. Hoblos, G. Barakat, G. (2017). Vibration-based Fault Diagnosis Approach for Permanent Magnet Synchronous Motors, *IFAC-PapersOnLine*, vol. 48, pp. 1444-1450.
7. Li, Y. Yi, C. Zhou, H. Yin, H. (2019). A novel feature extraction method based on discriminative graph regularized autoencoder for fault diagnosis, *IFAC-PapersOnLine*, vol. 52, pp. 272-277.
8. Wu, Y. Jiang, B. Wang, Y. (2020). Incipient winding fault detection and diagnosis for squirrel-cage induction motors equipped on CRH trains, *ISA Transactions*, vol. 99, pp. 488-495.
9. Zagirnyak, M. Mamchur, D. Kalinov, A. (2014). Induction motor diagnostic system based on spectra analysis of current and instantaneous power signals. *SOUTHEASTCON IEEE*.
10. Jesus A. Santos-Hernandez, Martin Valtierra-Rodriguez, Juan P (2019), Hilbert filter based FPGA architecture for power quality monitoring, *Measurement*, vol. 147.
11. Chen, J. Hu, W. Cao, D. (2019). An Imbalance Fault Detection Algorithm for Variable-Speed Wind Turbines: A Deep Learning Approach. *Energies*, vol. 12, pp. 2764.
12. Akar, M. Gercekioglu, H. (2017). Instantaneous power factor signature analysis for efficient fault diagnosis in inverter fed three phased induction motors, *International Journal of Hydrogen Energy*, vol. 42, pp. 8338-8345.
13. Watson, S. Xiang, B. Yang, W. (2010). Condition Monitoring of the Power Output of Wind Turbine Generators Using Wavelets. *IEEE Transactions on Energy Conversion*, vol. 25(3), pp. 715-721.
14. Frost, C. Morris, C. (2015). A. Mason-Jones, The effect of tidal flow directionality on tidal turbine performance characteristics. *Renewable Energy*, vol. 78, pp. 609-620.
15. Gu, F. Shao, Y. Hu, N. Naid, A. Ball, A.D. (2011). Electrical motor current signal analysis using a modified bispectrum for fault diagnosis of downstream mechanical equipment, *Mechanical Systems and Signal Processing*, vol. 25, pp. 360-372.